Research Article | Vol. 26, No. 20 | 1 Oct 2018 | OPTICS EXPRESS 26156
Optics EXPRESS

Nonlinear optical effects during femtosecond superradiant emission generation in semiconductor laser structures

PETER P. VASIL'EV,[1,2,*] RICHARD V. PENTY,[1] AND IAN H. WHITE[1]

[1]*Centre for Photonic Systems, Department of Engineering, University of Cambridge, 9 JJ Thomson Avenue, Cambridge, CB3 0FA, UK*
[2]*Quantum Electronics Division, PN Lebedev Physical Institute, 53 Leninsky Prospect, Moscow 119991, Russia*
**pv261@cam.ac.uk*

Abstract: This paper presents theoretical and experimental studies of ultrabright internal second harmonic during femtosecond superradiant emission generation in multiple sections GaAs/AlGaAs laser structures at room temperature. Experimentally measured conversion efficiencies are by 1-2 orders of magnitude greater than expected. To explain this fact, a model based on one-dimensional nonlinear Maxwell curl equations without taking into consideration the slowly-varying envelope approximation has been developed. It has been demonstrated that strong transient periodic modulation of e-h density and refraction index dramatically affects the process of superradiance in semiconductor media and can explain the ultrastrong internal second harmonic generation.

1. Introduction

Superradiance (SR) has been extensively studied for a long period of time since its invention in 1954 [1]. SR pulses have been observed in many types of media including gaseous, solid-state, polymer, and 0D, 2D, and 3D semiconductor devices [2–7]. Due to ultrafast characteristic times of electrons and holes in semiconductors, observable pulsewidths of SR pulses are in picoseconds and femtosecond ranges [2,4]. SR emission generated by semiconductor structures possesses a number of unique features, including ultrastrong internal second harmonic generation (SHG), superluminal pulse propagation [8], and greater coherence than lasing [9]. We have previously reported the generation of high-power femtosecond SR pulses from a number of semiconductor multiple contact laser devices at room temperature [2,4–9]. Such observations however have led to debate on whether the pulses generated are really akin to those superradiant phenomena observed in low temperature or low density structures, and whether they are different, for example, than those generated by conventional form of lasing. It has been recently demonstrated [8] that a characteristic feature of SR in semiconductors is strong coherent population $\lambda/2$ gratings burned by counter propagating femtosecond SR pulses in the e-h ensemble density. Due to a strong dependence of the refractive index on the carrier density in semiconductor materials, population gratings cause strong refractive index gratings which affect the propagation of SR pulses through the semiconductor. In addition, semiconductor materials exhibit strong quadratic nonlinearity and efficient SHG. A number of observations of internal SHG generation in GaAs and InGaAsP lasers were reported in the mid 1960's and 1980's [10–12]. Due to a very strong absorption coefficient γ exceeding 10^5 cm^{-1} at the SH wavelength in active layers of the lasers, the SHG output conversion efficiency is extremely low. The observed SHG power comes from the vicinity of the chip facet less or around the emission wavelength in depth. Since typical peak powers of SR pulses are much greater than these of lasing from the same devices, it is clear that SH should be larger when femtosecond SR pulses are generated. Indeed, we have observed bright blue emission from infrared GaAs/AlGaAs lasers under SR [13]. Furthermore, the intensity of SH and the efficiency of the frequency doubling proved to be by

#338398 https://doi.org/10.1364/OE.26.026156
Journal © 2018 Received 12 Jul 2018; revised 7 Sep 2018; accepted 9 Sep 2018; published 21 Sep 2018

Optics EXPRESS

1-2 orders of magnitude larger than that suggested by the theory of SHG. The phenomenon of the ultrabright SHG is important from both fundamental point of view and applications. It provides an additional evidence that SR is intrinsically different from lasing. It can be exploited for an efficient frequency doubling when other methods fail.

This paper presents further study of an influence of both population coherent grating and refractive index ones on the SR pulse generation. By comparing the results of modeling with the experimental data observed previously [2,4–9,13], one will clearly see that the formation of transient coherent e-h gratings can explain many features of SR, including unusually strong internal second harmonic generation and superluminal pulse propagation. The modelling shows that the periodic modulation of the nonlinear susceptibility of the medium during the SR pulse generation, caused by population and index gratings, is the most probable physical reason for a significant increase in the internal SHG efficiency. The model explains also why the efficiency of the internal SHG is so different for standard lasing and SR which is observed experimentally.

2. Experiment

A large variety of multiple section GaAs/AlGaAs bulk laser structures capable for the generation of SR emission were studied. In general, they had gain and saturable absorber sections of different geometries with different gain/absorber ratios and total cavity lengths. The devices under test were described in detail in our previous publications (see, for instance [2,13],). The composition of the GaAs/AlGaAs heterostructures varied a lot resulting in a broad range of the operating wavelengths between 820 and 890 nm. All devices can operate in c.w. lasing mode, gain/Q-switching or SR regimes depending on the driving conditions. Figure 1 presents microscopic view of two experimental samples having straight and tapered waveguides. A strong reverse bias of the central absorber section allows for frustrating the onset of lasing in the sample for a few nanoseconds and achieving much greater e-h densities than the threshold lasing density. At the appropriate driving conditions [4] SR phase transition occurs in the system and giant superradiant 200-400 femtosecond long pulses with peak powers of over 120-200 W are emitted.

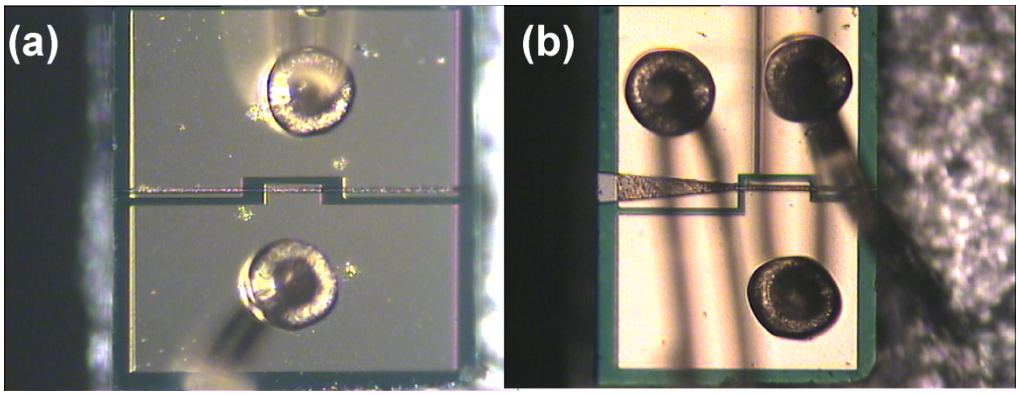

Fig. 1. Top view of experimental samples with straight (a) and tapered (b) active regions.

It has been observed that quite bright blue/violet emission is generated alongside with IR SR pulses. Figure 2 illustrates a typical SHG beam at around 442 nm which is emitted from the sample along with the collimated fundamental SR harmonic at 884 nm. The square blue filter shown in Fig. 2 blocks the fundamental beam and prevents an overexposure of the CCD detector. The laser was driven by 10 ns long current pulses with an amplitude of around 720 mA at the repetition rate of 10 MHz. The reverse bias was – 5.3 V. The maximum detected average power of the second harmonic was just under 0.2 μW at the fundamental average

Optics EXPRESS

power of about 1.92 mW. The measured SHG power varied a lot among the samples under test depending on parameters of the sample and driving conditions.

Fig. 2. SHG blue light beam from a GaAs/AlGaAs superradiant device as seen with a collimating lens through an optical filter. The fundamental harmonic average power was about 2 mW.

Figure 3 presents measured SH average power versus reverse bias V for 3 samples. The SH power is negligible at reverse biases below around V = 1.0-1.5 V. This corresponds to normal lasing in the devices.

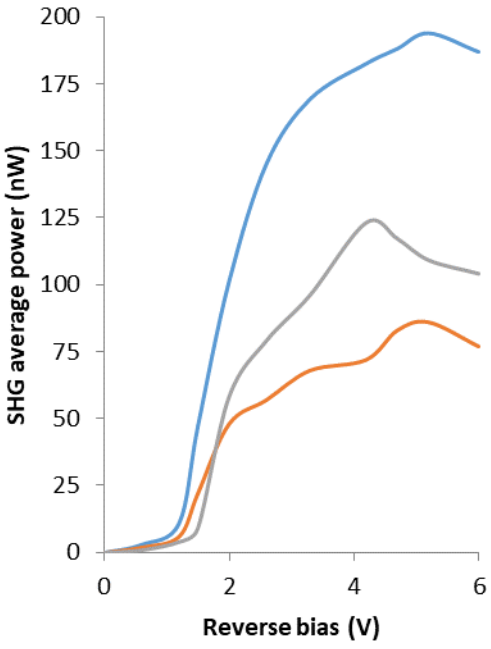

Fig. 3. SHG intensity versus reverse bias of 3 samples. The amplitude of the current pulses was 770 mA.

SR pulses are generated at larger V [2,4]. In general, the peak power and the number of SR pulses increases first with increasing V and the SHG intensity rises sharply. At certain V the number of SR pulses starts to drop rapidly and the SHG average power decreases. Similar

Optics EXPRESS

behaviour has been observed for all samples. Table 1 presents the result of the measurements of intensity of the first and second harmonics outside the samples. The conversion efficiency coefficient η (1/Watt) is determined by the relation $P_{2\omega} = \eta P_{\omega}^2$ [11,13].

Table 1. Measured the first and second harmonics intensities for different samples

Sample	Average P_{ω}	Average $P_{2\omega}$	η(1/W)	Description
H2-51	192mW	193nW	4.7×10^{-6}	250μm long, 5 μm straight
H2-31	9.2mW	104nW	1.1×10^{-7}	350μm long, 5 to 30 μm taper
H2-33	9.7mW	130nW	1.3×10^{-7}	350μm long, 5 to 30 μm taper
H2-52	2.3mW	36nW	6.2×10^{-7}	250μm long, 5 μm straight
H2-63	3.4mW	43nW	3.4×10^{-7}	350μm long, 5 μm straight
H2-112	3.2mW	41nW	3.6×10^{-7}	450μm long, 5 μm straight
H2-131	4.1mW	56nW	3.0×10^{-7}	450μm long, 5 μm straight

The values of η for SR pulses measured experimentally by more than the order of magnitude greater than these measured under standard lasing conditions and previously published in [10–12]. Indeed, the published values of η vary between 2.5×10^{-8} and 2.9×10^{-9} W^{-1}, whereas η in the Table 1 lies in the range of 4.7×10^{-6} and 1.1×10^{-7} W^{-1}. It should be noted that the values of η in Table 1 were calculated for the peak powers of the fundamental and the second harmonic femtosecond pulses outside the laser cavities. The internal SH power and SHG conversion efficiencies published in [10–12] were measured outside the cavities for c.w. or quasi-c.w. laser emission. In this case the peak and average powers were the same. That is why the comparison of the conversion efficiencies is correct since values of peak powers are used for all cases. Strictly speaking, values of the fundamental and second harmonics *inside* the cavities should be used for the estimation of η. However, the ratio of the second and first harmonic powers inside and outside the cavity is determined by the ratio of the corresponding refractive indices. The difference of the refractive indices leads to a correction of the calculated η by less than 15-20% for the values in Table 1 as well as calculated in [10–12].

The recorded intensity of SHG and the efficiency of the frequency doubling are by 1-2 orders of magnitude larger than that suggested by a conventional theory of SHG in bulk materials. One of possible explanations of this discrepancy is the presence of a weak refraction index periodicity of the active medium caused by transient population and index gratings which exist during SR emission generation [8]. We demonstrate that this fact can be confirmed by a theoretical model which takes into account both population and refractive index transient gratings.

3. Theoretical model

SR has been extensively studied theoretically in different media for many years [14–16]. Most of the models are based on solutions of semi classical or quantum Maxwell-Bloch equations. Because of the complexity of this treatment, the associated optical field equations have been traditionally simplified using several approaches, including the slowly-varying envelope approximation (SVEA) and rotating wave approximation (RWA). Our previous models of the SR generation in semiconductors [6,17,18] were also based on the first two approaches. It described reasonably well the basic properties of SR pulses. However, the approximations associated with these methods limit their range of applicability when ultrashort pulse phenomena and inhomogeneous media are considered. The finite-difference time-domain (FDTD) solution of the full-wave vectorial Maxwell–Bloch equations has been

Optics EXPRESS

previously used for the investigation of nonlinear gain spatio-temporal dynamics of active optical waveguides and semiconductor microcavities [19–21]. The interaction of the electromagnetic field with transient population gratings can result in significant deviations of experimentally observed SR pulses from results of models which treat the semiconductor as a spatially uniform medium. A model based on full Maxwell equations without the SVEA simplification can consistently take into account all features of the interaction of femtosecond SR pulses with the e-h system having a fine (λ/2) periodic spatial structure. This approach does not require splitting the optical field into counter-propagating waves as well as dividing the carrier density into continuous and spatially oscillating components as has been done in our previous model [8].

Assuming for simplicity that the medium is nonpermeable and isotropic, Maxwell's curl equations in one dimension are [22]

$$\frac{\partial H_y}{\partial t} = -\frac{\partial E_x}{\partial z}, \tag{1}$$

$$\frac{\partial D_x}{\partial t} = -\frac{\partial H_y}{\partial z} \tag{2}$$

$$E_x = \frac{D_x - (P_x^l + P_x^{nl})}{\varepsilon(z)} \tag{3}$$

where ε(z) is the relative permittivity of the medium and the polarization P_x consists of the linear and nonlinear terms

$$P_x = P_x^l + P_x^{nl} = \chi^{(1)} E_x + \chi^{(2)} E_x^2 \tag{4}$$

We treat semiconductor medium as a two-level system, because, as we have demonstrated before [4,23], during the early stages of the development of SR pulses almost all electrons and hole condense in the phase space at the band gap. As opposed to case of lasing and spontaneous emission when e-h pairs are located over a broad energy range within the conductive and valence bands, SR pulses originate from the recombination of e-h pairs located within a narrow band at the band gap energy [23]. There is negligible emission from upper energy levels, and so the density matrix formalism for a two-level system is valid. The Bloch equations for the elements of the density matrix are [19]

$$\frac{\partial u}{\partial t} = \omega_0 v - \frac{u}{T_2}, \frac{\partial v}{\partial t} = -\omega_0 u + 2\frac{d}{\hbar} E_x w - \frac{v}{T_2}, \frac{\partial w}{\partial t} = -2\frac{d}{\hbar} E_x v - \frac{w - w_0}{T_1} \tag{5}$$

The components *u* and *v* represent, respectively, the dispersive or in-phase and the absorptive or in-quadrature polarization components associated with the dipole transition. The polarization of the two-level medium is determined by the relation $\mathrm{Px(t)} = -\mathrm{ndu(t)}$, where *d* is the transition dipole moment, and *n* is the e-h density. The component *w* represents the fractional population difference in the two-level system states and T_1 is the e-h spontaneous lifetime. Due to a strong dependence of the refractive index on carrier density in semiconductor media, a transient spatial population grating results in a corresponding refractive index grating. We have included this effect by an introduction of a parameter which is proportional to the linewidth enhancement factor α of the semiconductor structure [24,25]. This factor is defined as

$$\alpha = -\frac{\partial Re\chi^{(1)}(\omega)/\partial n}{\partial Im\chi^{(1)}(\omega)/\partial n} \tag{6}$$

Optics EXPRESS

The real and imaginary parts of $\chi^{(1)}$ are related to the refractive index and optical gain, respectively. The physical origin of α lies in the asymmetric nature of electron and hole distributions in semiconductors. The value of α depends on many factors, including the material parameters of the semiconductor, frequency shift with respect to the optical gain peak, excitation level, device geometry, etc. By contrast to gaseous and solid-state media where α is negligible, it can be far greater than 10 in bulk GaAs/AlGaAs heterostructures at photon energies close to the band gap [25]. We calculated the relevant values of α for each wavelength shift (depending on bias V) and each value of the carrier density using the approach by Vahala et al [25].

The full-wave vector Maxwell's equations coupled to the time evolution equations of the two-level quantum system are discretized using the Yee, staggered-grid finite difference algorithm for Maxwell's equations [26]. The system is solved numerically in the time domain by the standard leapfrog time-advancing scheme (FDTD). We used the same algorithm for the numerical solution of the equations as described elsewhere [19–21]. At each time step, the Courant stability criterion $c\Delta t / \Delta z \le 1$ is fulfilled in the manner described in [19]. We have used very fine discretization in space in order to spatially resolve λ/2 gratings. The boundary conditions and field reflections at the chip facets are automatically taken into account by the spatial profile of the dielectric constant $\varepsilon(z)$. The modification of the numerical algorithm can be easily performed since the FDTD calculation scheme of Yee has already been adapted to several nonlinear problems of electromagnetism such as the propagation of solitons [27], the self-focusing of beams [28], and the SH generation [22]. The model was calibrated in such a way that the peak power of the first harmonic SR pulses and their durations was approximately equal to the measured experimental data at given driving current amplitudes and reverse biases V.

Figures 4, 5, and 6 illustrate the results of calculations. The spatial evolution in time of the electromagnetic field (the first and second harmonics) and the carrier density and refractive index was calculated. Since the all variables have a very fine sub-μm spatial structure, it was impossible to plot clearly the spatial distribution over the full length of the sample. As mentioned above, the SH is effectively generated at the facets of the devices. Thus, the calculated distributions of all variables inside the structure are plotted for the last 2-3 microns at the chip facet where SHG has maximum intensity (see Fig. 5 below). The carrier density and the fundamental harmonic have a sine/cosine-like distribution with a λ/2 and λ periodicity, respectively. The SH electric field has a more complex spatial structure due to the interaction with the transient population grating.

As mentioned above, observed SH power primarily comes from the vicinity of the chip facet due to its large absorption of the semiconductor. Figure 5 presents a typical snap-shot of the fundamental and SH powers at the facet during an SR pulse generation.

Optics EXPRESS

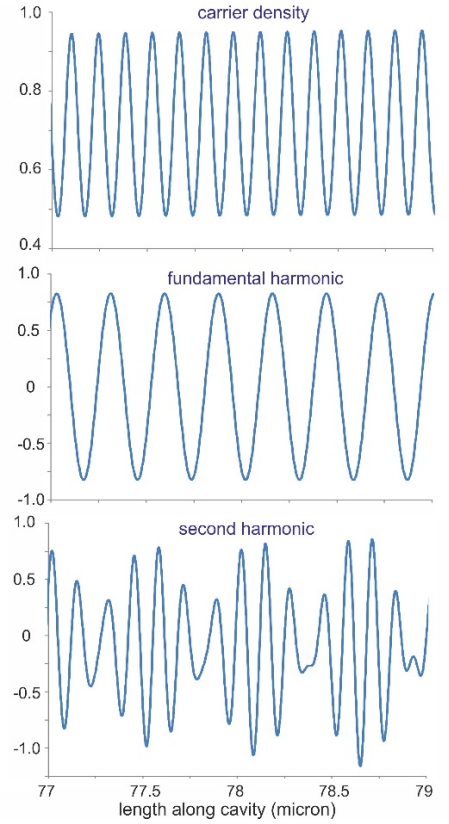

Fig. 4. A snap-shot of the calculated distribution of the carrier density, fundamental and second harmonic fields at a certain time during the SR pulse generation. The vertical axis is plotted in the arbitrary units.

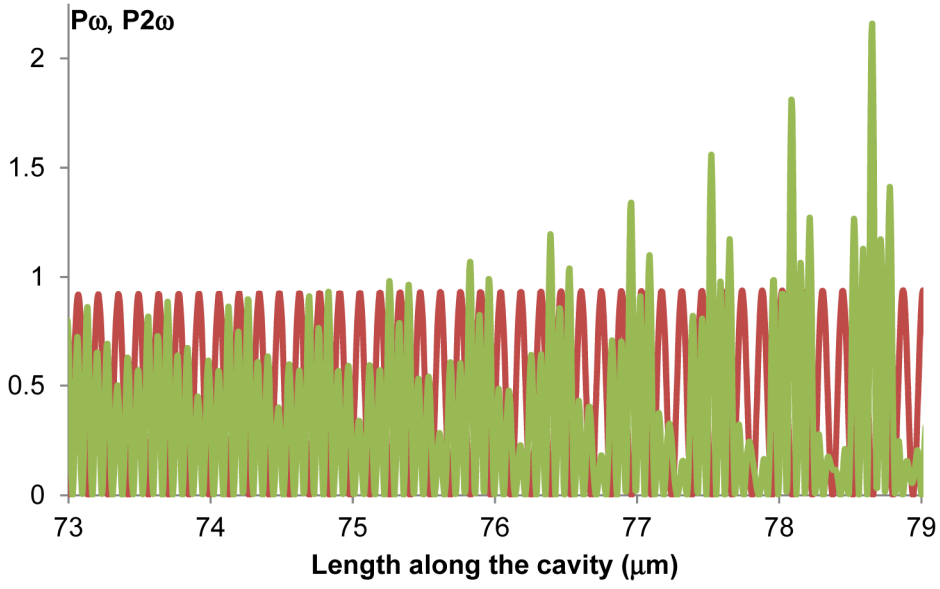

Fig. 5. Calculated distribution of the fundamental (red) and second harmonic (green) powers at the chip end.

Optics EXPRESS

As one expects, the SH intensity grows rapidly towards the facet. The maximum power and the SHG conversion efficiency is strongly affected by transient population and index gratings existing inside the sample. It is expected that the SH power and the conversion efficiency should increase with increasing the initial e-h density at the very beginning of an SR pulse evolution. The transient gratings are much more pronounced at greater values of n. Figure 6 shows dependences of the SH peak intensity versus the fundamental peak power and initial e-h density. For relatively small values of P_ω the SH power follows the conventional law $P_{2\omega} \propto P_\omega^2$. However, at larger $P\omega$ the SH intensity increases more rapidly. This is because the peak power of the fundamental harmonic depends strongly on the initial carrier density. At the same time, the strength of both transient population and index gratings increases with carrier density as well. The maximum calculated amplitude of the carrier density variation can be as large as 6 x 10^{18} cm^{-3}, the corresponding refractive index variations being of about 10^{-2} [13].

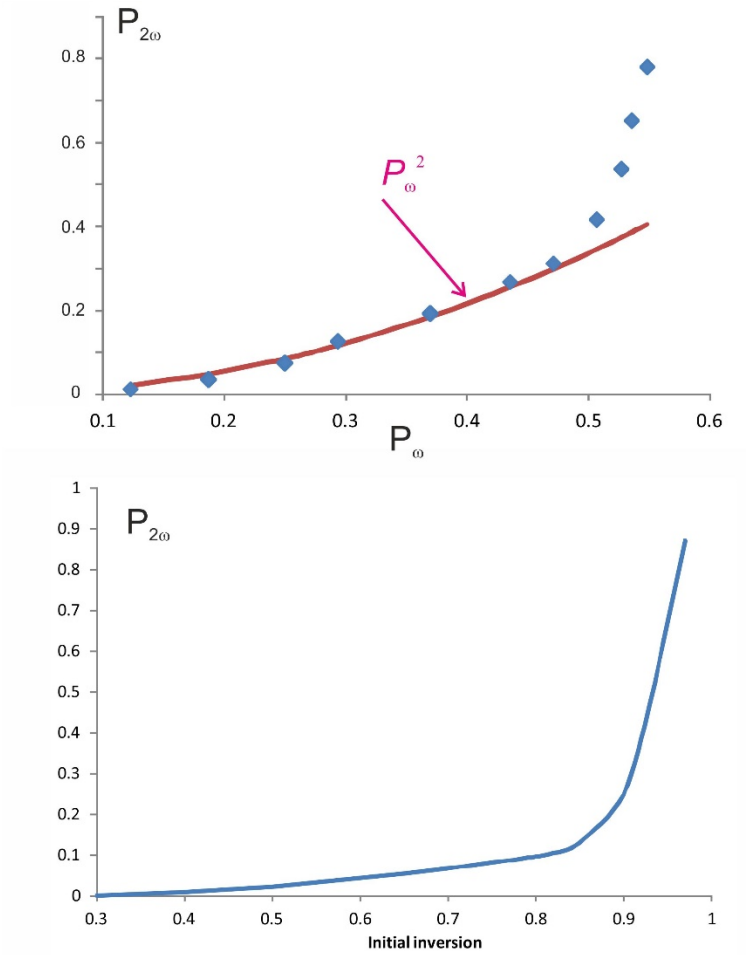

Fig. 6. Calculated normalized intensity of the internal SHG intensity versus peak fundamental power (top) and initial inversion (bottom).

We attribute the enormous enhancement of the efficiency of the SH generation to the interaction of the electromagnetic field with population and index gratings which are built up in the semiconductor medium during the SR emission generation.

Optics EXPRESS

4. Discussion

Internal SH intensity can be easily calculated since SHG has been one of the most studied phenomena in nonlinear optics and the theory of SHG is well-known. The SH intensity is derived from a wave equation for the electromagnetic field $E_{2\omega}$.Without depletion of Eω propagating in z direction it reads

$$\frac{\partial E_{2\omega}}{\partial z} = -\frac{i\omega}{\mu_{2\omega} c} d_{eff} E_{\omega}^2 e^{i\Delta kz} - \gamma E_{2\omega} \tag{7}$$

where d_{eff} is the effective nonlinear coefficient, Δk is the phase mismatch, $\mu_{2\omega}$ is the refractive index at the SH wavelength, and c is the velocity of light. The solution of the equation can be readily found and

$$\left|E_{2\omega}\right|^2 \propto \frac{E_{\omega}^4}{\Delta k^2 + \gamma^2}\left\{\left(\cos \Delta kz - e^{-\gamma z}\right)^2 + (\sin \Delta kz)^2\right\} \tag{8}$$

Since $\gamma >> 10^5$ cm^{-1}, the SH intensity saturates at distances < 1 μm. For GaAs one has d_{eff} = 2.0 x10^{-10} m/V, μ_{ω} = 3.62, $\mu_{2\omega}$ = 5.04, γ = 2.83x10^7 m^{-1} at the SH wavelength of 440 nm. The solution of Eq. (7) with (8) gives for the SH intensity $I_{2\omega} = c\varepsilon_0 \mu_{2\omega} \left|E_{2\omega}\right|^2 / 2$ (in W/m^2)

$$I_{2\omega} = \eta I_{\omega}^2 = \frac{8\pi^2 d_{eff}^2}{\mu_{2\omega}\mu_{\omega}^2 c \lambda_{\omega}^2 \varepsilon_0 (\Delta k^2 + \gamma^2)} I_{\omega}^2 \tag{9}$$

This gives the value η = 8 x 10^{-9} W^{-1} in our case of the emission area of around 2.5x10^{-12} m^2. As presented in Table 1, the measured SH power and conversion efficiency is 1-2 orders of magnitude greater than the calculated value.

The exact physical reason behind the ultra strong SHG under SR generation is unclear at the moment. However, one of the possible causes of this effect is an existence of periodic modulation of the e-h density and strong transient population and index gratings which associate the process of SR in semiconductor media. By contrast to standard lasing, when the population grating also exists and the typical modulation of the e-h density is a few percent only, the modulation of e-h density approaches 100% when SR pulses are generated. It has been previously found [8] that coherent transient gratings strongly affect the group refractive index of the medium and cause the superluminal propagation of SR pulses.

A refractive index grating can significantly alter the phase-matching condition of the nonlinear wave interaction. It may permit effective SHG even if the phase-matching condition is not satisfied in a uniform medium of the same background refractive indices at the fundamental and SH frequencies. This phenomenon was first investigated many years ago [29]. A periodic grating rephases the nonlinear polarization and the generated electromagnetic waves. Strong periodic λ/2 modulation of the e-h density and corresponding modulation of the refractive index can result in quasi phase matching conditions in a similar manner as in periodically poled materials used for frequency doubling. In addition, it has been shown that even a weak spatial periodic modulation of the order of the wavelength of the nonlinear susceptibility $\chi^{(2)}$ of a medium leads to a remarkable enhancement of the SH conversion efficiency [30]. It has been demonstrated that a periodic variations of the refractive index ~10^{-3} – 10^{-2} can result in an increase of the SHG efficiency by more than an order of magnitude at appropriate conditions. Moreover, it has been experimentally proved [31] that the SHG conversion efficiency is enhanced in a periodically stratified GaAs/AlGaAs structures as compared to a spatially uniform medium of the same composition.

It is reasonable to suggest that the periodic modulation of the nonlinear susceptibility of the medium during the SR pulse generation, caused by population and index gratings, leads to a significant (experimentally observed) increase in the internal SHG efficiency. A λ/2 transient grating of the refraction index distorts the natural dispersion of the material in a

Optics EXPRESS

similar manner to 1D photonic crystals. As a result, the efficiency of the harmonic doubling is strongly enhanced. A similar effect has been reported by de Ceglia et al [32] who demonstrated a drastically enhanced SHG in a 1D GaAs subwavelength resonant grating under an external optical pumping. The coupling of the pump field to guided mode resonances produced by the grating introduces sharp, Fano-like resonances where strong field localization and enhancement take place, leading to the prediction of SHG conversion efficiencies that are 4–5 orders of magnitude larger than in bulk structures.

The developed model can be used for the simulation of the SR generation in other types of resonators, for example ring cavities, Fabry-Perrot cavities with antireflection coatings, or lasers where refractive index gratings are formed on purpose (DFB or DBR semiconductor lasers). It should be noted, however, that the simple presence of a periodic modulation of the refractive index is not sufficient for enhancing of the internal SHG. The period of the spatial modulation and its amplitude should be appropriately chosen. The present model allows for accurate calculations of those parameters and proper design of laser cavities for achieving the ultimate parameters of SR pulses and maximum intensities of SHG.

5. Conclusion

In summary, we have presented experimental and theoretical studies of the generation of ultrabright internal second harmonic during SR emission generation in semiconductor laser structures. Typical experimentally measured conversion efficiencies proved to be by 1-2 orders of magnitude greater than those previously reported in semiconductor lasers based on bulk and quantum-well materials. A model based on nonlinear one-dimensional Maxwell curl equations without taking into consideration the slowly-varying envelope approximation has been developed. The model takes into account a deep $\lambda/2$ modulation of the carrier density and corresponding modulation of the refractive index and nonlinear susceptibility and describes well the evolution of femtosecond SR pulses. The formation of transient coherent population and refractive index gratings can explain many features of SR, including unusually strong internal second harmonic generation and superluminal pulse propagation which has been observed previously.

Acknowledgments

The authors would like to thank H.Kan and H.Ohta for the fabrication of the samples and M. Scalora for valuable comments.

References

1. R. H. Dicke, “Coherence in spontaneous radiation processes,” Phys. Rev. **93**(1), 99–110 (1954).
2. P. P. Vasil’ev, R. V. Penty, and I. H. White, “Superradiant emission in semiconductor diode laser structures,” IEEE J. Sel. Top. Quantum Electron. **19**(4), 1500210 (2013).
3. K. K. Cong, Q. Zhang, Y. R. Wang, G. T. Noe, A. Belyanin, and J. Kono, “Dicke superradiance in solids,” J. Opt. Soc. Am. B **33**(7), C80–C101 (2016).
4. P. P. Vasil’ev, “Femtosecond superradiant emission in inorganic semiconductors,” Rep. Prog. Phys. **72**(7), 076501 (2009).
5. M. Xia, R. V. Penty, I. H. White, and P. P. Vasil’ev, “Femtosecond superradiant emission in AlGaInAs quantum-well semiconductor laser structures,” Opt. Express **20**(8), 8755–8760 (2012).
6. D. L. Boiko and P. P. Vasil’ev, “Superradiance dynamics in semiconductor laser diode structures,” Opt. Express **20**(9), 9501–9515 (2012).
7. V. F. Olle, P. P. Vasil’ev, A. Wonfor, R. V. Penty, and I. H. White, “Ultrashort superradiant pulse generation from a GaN/InGaN heterostructure,” Opt. Express **20**(7), 7035–7039 (2012).
8. P. P. Vasil’ev, R. V. Penty, and I. H. White, “Pulse generation with ultra-superluminal pulse propagation in semiconductor heterostructures by superradiant-phase transition enhanced by transient coherent population gratings,” Light Sci. Appl. **5**(6), e16086 (2016).
9. P. P. Vasil’ev, V. Olle, R. V. Penty, and I. H. White, “Long-range order in a high-density electron-hole system at room temperature during superradiant phase transition,” Europhys. Lett. **104**(4), 40003 (2013).
10. M. D. Malmstrom, J. J. Schlikman, and R. H. Kingstron, “Internal second-harmonic generation in gallium arsenide lasers,” J. Appl. Phys. **35**(1), 248–249 (1964).

Optics EXPRESS

11. N. Ogasawara, R. Ito, H. Rokukawa, and W. Katsurashima, "Second harmonic generation in an AlGaAs double-heterostructure laser," Jpn. J. Appl. Phys. **26**(8), 1386–1387 (1987).
12. H. Kanamori, S. Takashima, and K. Sakurai, "Near-infrared diode laser spectrometer with frequency calibration using internal second harmonics," Appl. Opt. **30**(27), 3795–3798 (1991).
13. P. P. Vasil'ev, H. Kan, H. Ohta, R. V. Penty, and I. H. White, "Anomalous second harmonic generation during femtosecond superradiant emission from GaAs/AlGaAs laser structures," in Proc. 25nd IEEE Int. Semiconductor Laser Conf. (ISLC), Kobe, Japan (2016).
14. M. Gross and S. Haroche, "Superradiance: an essay on the theory of collective spontaneous emission," Phys. Rep. **93**(5), 301–396 (1982).
15. J. C. MacGillivray and M. S. Feld, "Theory of superradiance in an extended, optically thick medium," Phys. Rev. A **14**(3), 1169–1189 (1976).
16. J. J. Maki, M. S. Malcuit, M. G. Raymer, R. W. Boyd, and P. D. Drummond, "Influence of collisional dephasing processes on superfluorescence," Phys. Rev. A Gen. Phys. **40**(9), 5135–5142 (1989).
17. P. P. Vasil'ev, "Role of a high gain of the medium in superradiance generation and in observation of coherent effects in semiconductor lasers," Quantum Electron. **29**(10), 842–846 (1999).
18. P. P. Vasil'ev and I. V. Smetanin, "Condensation of electron-hole pairs in a degenerate semiconductor at room temperature," Phys. Rev. B **74**(12), 125206 (2006).
19. G. M. Slavcheva, J. M. Arnold, and R. W. Ziolkowski, "FDTD simulation of the nonlinear gain dynamics in active optical waveguides and semiconductor microcavities," IEEE J. Sel. Top. Quantum Electron. **10**(5), 1052–1062 (2004).
20. A. S. Nagra and R. A. York, "FDTD analysis of wave propagation in nonlinear absorbing and gain media," IEEE Trans. Antenn. Propag. **46**(3), 334–340 (1998).
21. J. A. Gruetzmacher and N. F. Scherer, "Finite-difference time-domain simulation of ultrashort pulse propagation incorporating quantum-mechanical response functions," Opt. Lett. **28**(7), 573–575 (2003).
22. R. M. Joseph and A. Taflove, "FDTD Maxwell's equations models for nonlinear electrodynamics and optics," IEEE Trans. Antenn. Propag. **45**(3), 364–374 (1997).
23. P. P. Vasil'ev, "Conditions and possible mechanism of condensation of e-h pairs in bulk GaAs at room temperature," Phys. Status Solidi **241**(6), 1251–1260 (2004).
24. P. Vasil'ev, *Ultrafast diode lasers: fundamentals and applications* (Artech House, Norwood, 1995).
25. K. Vahala, L. C. Chiu, S. Margalit, and A. Yariv, "On the linewidth enhancement factor in semiconductor injection lasers," Appl. Phys. Lett. **42**(8), 631–633 (1983).
26. K. S. Yee, "Numerical solution of initial boundary value problems involving Maxwell's equations in isotropic media," IEEE Trans. Antenn. Propag. **14**(3), 302–307 (1966).
27. A. Bourgeade and E. Freysz, "Computational modelling of second-harmonic generation by solution of full-wave vector Maxwell equations," J. Opt. Soc. Am. B **17**(2), 226–234 (2000).
28. R. W. Ziolkowski and J. B. Judkins, "Full-wave vector Maxwell equation modeling of the self-focusing of ultrashort optical pulses in a nonlinear Kerr medium exhibiting a finite response time," J. Opt. Soc. Am. B **10**(2), 186–198 (1993).
29. N. Bloembergen and A. J. Sievers, "Nonlinear optical properties of periodic laminar structures," Appl. Phys. Lett. **17**(11), 483–486 (1970).
30. J. W. Haus, R. Viswanathan, M. Scalora, A. G. Kalocsai, J. D. Cole, and J. Theimer, "Enhanced second-harmonic generation in a media with a weak periodicity," Phys. Rev. A **57**(3), 2120–2128 (1998).
31. J. P. van der Ziel and M. Ilegems, "Optical second harmonic generation in periodic multilayer GaAs-$Al_{0.3}Ga_{0.7}As$ structures," Appl. Phys. Lett. **28**(8), 437–439 (1976).
32. D. de Ceglia, G. D'Aguanno, N. Mattiucci, M. A. Vincenti, and M. Scalora, "Enhanced second-harmonic generation from resonant GaAs gratings," Opt. Lett. **36**(5), 704–706 (2011).